Journal Name

Dynamic Article Links ►

Cite this: DOI: 10.1039/c0xx00000x

www.rsc.org/xxxxxx

ARTICLE TYPE

Facile synthesis of a bulky BPTPA donor group suitable for cobalt electrolyte based dye sensitized solar cells

Peng Gao,[a] Yongjoo Kim,[ab] Jun-Ho Yum,[a] Thomas W. Holcombe,[a] Mohammad K. Nazeeruddin,[a] and Michael Grätzel[a]

Received (in XXX, XXX) Xth XXXXXXXXX 20XX, Accepted Xth XXXXXXXXX 20XX
DOI: 10.1039/b000000x

An efficient synthesis of N-(2',4'-bis(hexyloxy)-[1,1'-biphenyl]-4-yl)-N-(4-bromophenyl)-2',4'-bis (hexyloxy) -[1,1'-biphenyl]-4-amine (BPTPA donor, **5**) was developed. The four-step reaction with much improved yield decreased the cost dramatically at the same time. Based on the new synthetic route, **NT35** and **G220** containing BPTPA and exhibiting different IPCE spectrum response were synthesized. **G221** with just a TPA as the donor unit was also made for comparison reason. The combination of the sensitizers bearing BPTPA donor with cobalt complex showed higher J_{sc}, V_{oc} and better visible light spectrum response than that of the combinations with Iodine electrolyte. The BPTPA donor could efficiently suppress the electron recombination between the TiO_2 surface and the redox oxide species and therefore can fully take the advantage of the high V_{oc} brought by the cobalt electrolyte. Among these sensitizers, **G220** showed the best photovoltaic performance: a short-circuit photocurrent density (J_{sc}) of 14.8 mA cm^{-2}, an open-circuit photovoltage (V_{oc}) of 0.87 V, and a fill factor (*FF*) of 0.71, corresponding to an overall conversion efficiency of 9.06% under standard global AM 1.5 solar light condition. The result shows that the organic sensitizers based on this bulky BPTPA donor are promising candidates for cobalt-based DSSCs.

Introduction

Donor-π-bridge–acceptor (D-π-A) organic dyes for dye sensitized solar cells (DSSCs) have been the subject of much academic and industrial research, owing to their wide variety, high molar extinction coefficients and potentially low cost of fabrication compared with ruthenium dye sensitizers.[1] Among the various organic donors, e.g., triphenylamine,[2] coumarin,[3] indoline,[4], fulvenyl,[5] and 4H-pyran-4-ylidene,[6] that have been explored in DSCs, triphenylamine (TPA) and its derivatives are the most universally utilized. Recently, one triphenylamine-based dye has yielded a record high efficiency of 10.3% (AM 1.5G condition).[7] Theoretical and experimental studies have demonstrated that TPA unit is expected to greatly confine the cationic charge from the semiconductor surface and efficiently hamper the recombination. TPA also shows a huge steric hindrance and can therefore prevent unfavorable dye aggregation at the semiconductor surface.[8] At the same time, it is found that among the reported organic sensitizers for liquid electrolyte based DSCs, those based on the TPA moiety are more suitable for solid state DSCs, due to the excellent electron-donating nature and non-planar configuration of TPA.[9] The intrinsic hole conducting capability of the TPA units can improve the wetting of spiro-OMeTAD resulting in fast charge transfer in solid state DSCs.[10] Structure modification has further brought vitality to TPA as a donor fragment, eg. alkyl or alkyloxy substitution,[11] fusion of aromatic rings,[12] planarization[13] etc.

Besides the classic iodide/triiodide (I_3^-/I^-) redox shuttle and among the many new redox species under study,[14] divalent/trivalent cobalt bipyridine complexes ($[Co(bpy)_3]^{3+/2+}$) exhibit the most impressive performance. The advantages of using cobalt complex redox shuttle as electrolyte including variability of the chemical structure, tunability of the redox potential and transparency to visible light. Despite these merits, however, after the first report in 2001 by Nusbaumer et al.[15] few papers have been published on cobalt complex redox shuttles in DSSCs,[16] mainly due to the lack of proper dye sensitizer to compile with the new electrolyte. People also found that when the cobalt complexes were made with the same dye molecules, which work well with iodine, the efficiencies achieved were rather poor.[17] Only a few examples have been shown that the dye molecules gave improved efficiency in cobalt complexes than that of iodine electrolyte.[16b-d]

Recently, one D-π-A dye called **D35** was synthesized by modifying normal TPA donor with substitution of bis(butoxyl)benzene.[18] (Figure 1) Hagfeldt et al have found that **D35** performed very well with cobalt-based mediators due to the efficient suppression of recombination by the extra bulky bis(alkyloxy)phenyl on the TPA moiety with overall conversion efficiencies of 6.7%.[19] To further explore the validity of the so called BPTPA donor (shown as bold structure in **Figure 1**), our group further synthesized dye **Y123** with much extended spectral response. Therefore the dye afforded an improved efficiency of

8.8% with cobalt based redox system,[20] and further improvement to 10% by optimizing TiO_2 mesoporous film[21] or new cobalt bipyridine pyrazole electrolyte.[16c] Later on, **Y123** was applied as a cosensitizer with a porphyrin chromophore yielding an efficiency of 12.3% and again used in conjunction with the $[Co(bpy)_3]^{3+/2+}$ redox couple.[22] All these examples indicated that the D-π-A dyes with BPTPA donor are compatible with cobalt redox mediators, which are promising alternatives to the I_3^-/I^- redox couple for large-scale manufacturing of DSCs due to the reason mentioned above.[23]

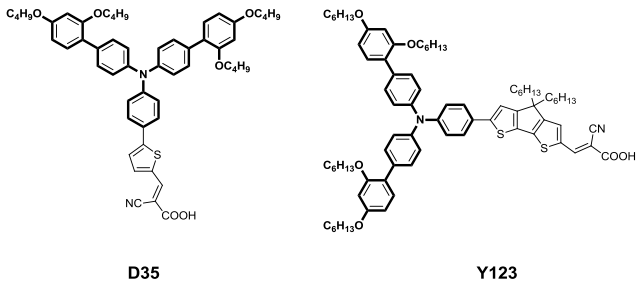

Figure 1. Structures of **D35** and **Y123** (BPTPA donor in bold)

So far the synthesis of D-π-A dyes with BPTPA donor went mainly two different routes. First one is the in situ installation of the donor moiety[18] while the second one needs pre-synthesis of the donor before it is connected to a desired π bridge.[20] The utilization of the first route is confined to a few stable intermediate compounds. Although the premade BPTPA donor is easily popularized and readily used with high versatility, the current synthetic route towards premade donor is, however, expensive and tedious which will limit its large-scale application.[20]

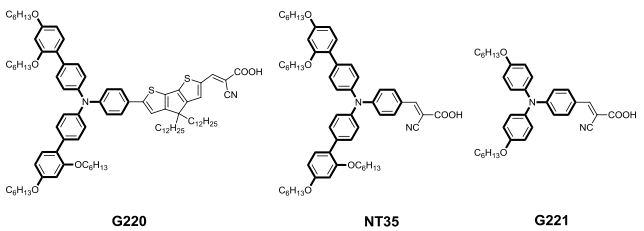

Figure 2. Structures of synthesized dyes

For the purpose of a convenient synthesis and scale up of the BPTPA donor, in this work, we will report newly designed synthetic route to the donor moiety before it is applied to construct new dye sensitizers. To further widen the scope of this donor group, (*E*)-3-(4-(bis(2',4'-bis(hexyloxy)-[1,1'-biphenyl]-4-yl)amino)phenyl)-2-cyanoacrylic acid (**NT35**) and (*E*)-3-(6-(4-(bis(2',4'-bis(hexyloxy)-[1,1'-biphenyl]-4-yl)amino)phenyl)-4,4-di-dodecyl-4H-cyclopenta[1,2-*b*:5,4-*b'*]dithiophen-2-yl)-2-cyano-acrylic acid (**G220**) are synthesized bearing the same BPTPA donor and cyanoacrylic acid as electron acceptor and anchoring group. The performances of these dyes with cobalt redox couple are systematically studied and compared with those with I_3^-/I^- redox couple. To show the effectiveness of the BPTPA donor in slowing down recombination rate in both electrolytes, a simple version of **NT35**, (*E*)-3-(4-(bis(4-(hexyloxy)phenyl)amino) phenyl)-2-cyanoacrylic acid (**G221**) is also synthesized according to reported similar procedure.[24] (Figure 2)

Experimental

Materials

All commercially obtained reagents were used as received: 4-Chlororesorcinol (Aldrich SA), bis(pinacolato)diboron (Combi-Blocks Inc.), bis(4-bromophenyl)amine (Aldrich), 4-Bromobenzaldehyde and 1-bromo-4-iodobenzene (Alfa Aesar). Anhydrous N,N-dimethylformamide (DMF) (AcroSeal) and anhydrous tetrahydrofuran (THF) (AcroSeal) were obtained from Acros and used as received. Thin-layer chromatography (TLC) was conducted with Merck KGaA precoated TLC Silica gel 60 F254 aluminum sheets and visualized with UV and potassium permanganate staining. Flash column chromatography was performed on glass columns packed with silica gel using Silicycle UltraPure SilicaFlash P60, 40-63 μm (230-400 mesh). 1-chloro-2,4-bis(hexyloxy)benzene [25], 6-bromo-4,4-didodecyl-4H-cyclopenta[1,2-*b*:5,4-*b'*]dithiophene-2-carbaldehyde[11b], bis(4-(hexyloxy)phenyl)amine[26], were synthesized according similar or modified literature procedures. Transparent FTO conducting glass (fluorine doped SnO_2, NSG, sheet resistance 10 Ω per square) was obtained from Nippon Sheet Glass.

Instrumentation

^{1}H-NMR spectra and proton-decoupled ^{13}C-NMR spectra were recorded on a Bruker Avance-400 (400 MHz), Bruker Avance III-400 (400MHz), or Bruker DPX-400 (400 MHz) spectrometer and are reported in ppm using solvent as an internal standard ($CDCl_3$ at 7.26 ppm and 77.23 ppm, CD_2Cl_2 at 5.32 ppm and 53.8 ppm). High-resolution mass spectra were obtained at the École Polytechnique Fédérale de Lausanne mass spectrometry laboratory (EPFL). Optical measurements were carried out in 1 cm cuvettes with Merck Uvasol grade solvents. UV-Vis spectra were measured with a Hewlett Packard 8453 UV-Vis spectrometer. Cyclic voltammetry was measured with an Autolab Eco Chemie cyclic voltammeter in a three-electrode single-compartment cell with a glassy carbon working electrode, a platinum wire counter electrode, and a platinum wire reference electrode. All potentials were internally referenced to the ferrocene/ferrocenium couple.

Synthesis

2-(2,4-bis(hexyloxy)phenyl)-4,4,5,5-tetramethyl-1,3,2-dioxa borolane (2). In a 100 mL single-neck round-bottom flask, 8.56 grams of bishexyloxy-4-chloro-resorcinol (27.36 mmol), 10.42 grams of bis(pinacolato)diboron (41.03 mmol), and 8.06 grams potassium acetate (82.12 mmol) were dissolved in 60 mL of dioxane. This solution was degassed for 20 minutes with a stream of N_2, after which time 10 mg of Pd_2dba_3 and 20 mg of X-Phos were added simultaneously, in one batch. The reaction was then brought to 95 °C for 10 hours. The reaction was then cooled to RT, and plugged through a thin pad of $MgSO_4$ with DCM. The crude product was purified with gradient silica gel chromatography: 100% hexanes to 20:80 Hex:DCM. 6.23 grams (70% yield) of a pure clear oil was obtained. ^{1}H NMR (400 MHz, CD_2Cl_2) δ 7.54 (d, *J* = 8.2 Hz, 1H), 6.46 (dd, *J* = 8.2, 2.2 Hz, 1H), 6.40 (d, *J* = 2.2 Hz, 1H), 3.96 (dt, *J* = 14.4, 6.4 Hz, 4H), 1.85 – 1.72 (m, 4H), 1.61 – 1.42 (m, 4H), 1.41 – 1.34 (m, 8H), 1.32 (s, 12H), 0.99 – 0.86 (m, 6H) ppm. ^{13}C NMR (100 MHz, CD_2Cl_2) δ = 165.58, 163.11, 137.71, 129.65, 105.10, 99.20, 83.17, 82.81,

68.20, 67.88, 31.66, 31.58, 29.32, 29.20, 25.68, 25.67, 24.83, 24.64, 22.71, 22.60, 13.88, 13.80 ppm.

Bis(2',4'-bis(hexyloxy)-[1,1'-biphenyl]-4-yl)amine (3). A solution of bis(4-bromophenyl)amine (740 mg, 2.26 mmol) and **2** (2 g, 4.954 mmol) in toluene (24 ml) and K_2CO_3 solution 2M (8 ml) was stirred at room temperature with N_2 bubbling for 30 minutes. $Pd(PPh_3)_4$ (50 mg, 0.045 mmol) was then added, followed by freeze-pump-thaw degassing procession. The resulting reaction mixture was heated at 100 °C for 20 h. After cooling to room temperature, the reaction mixture was extracted with CH_2Cl_2. The combined layers were washed with brine and dried over anhydrous magnesium sulfate. Concentration under vacuum followed by silica gel column chromatography using an eluent gradient of hexane: dichloromethane (final ratio 1:1) afforded **3** as a light yellow waxy solid (1.47 g, 90%). ^{1}H NMR (400 MHz, CD_2Cl_2) δ 7.49 (d, *J* = 8.2 Hz, 4 H), 7.29 (d, *J* = 8.2 Hz, 2 H), 7.17 (d, *J* = 8.2 Hz, 4 H), 6.59 (d, *J* = 8.2 Hz, 4 H), 5.96 (s, 1 H), 4.01 (m, 8 H), 1.82 (m, 9 H), 1.45 (m, 26 H), 0.96 (m, 12 H) ppm. ^{13}C NMR (101 MHz, CD2Cl2) δ 159.5, 157.0, 141.5, 130.6, 130.3, 130.2, 123.0, 117.0, 105.3, 100.2, 68.4, 68.1, 31.7, 31.5, 29.4, 29.2, 25.8, 22.7, 13.9 ppm. HRMS (MALDI-TOF), m/z (M^+): for $C_{48}H_{67}NO_4$ calculated 721.5070; found 721.5065.

N-(2',4'-bis(hexyloxy)-[1,1'-biphenyl]-4-yl)-N-(4-bromo phenyl)-2',4'-bis(hexyloxy)-[1,1'-biphenyl]-4-amine (5). Potassium tert-butoxide (116 mg, 1.03 mmol) was added to a 100 mL round-necked flask containing 3 (500 mg, 0.692 mmol), 1-bromo-4-iodobenzene (235 mg, 0.832 mmol), and CuI (13.3 mg, 0.07 mmol) under a flow of argon, and then (±)-trans-1,2-diaminocyclohexane (15.65 mg, 0.137 mmol) and 1,4-dioxane (20 mL) were added with syringe in sequence. The mixture was heated to 110°C with good stirring overnight under argon atmosphere. After cooling, H2O (100 mL) was added, and the mixture was extracted with CH_2Cl_2. The organic layer was combined and washed with H_2O and then dried over anhydrous Na_2SO_4. After the solvent was evaporated, the residue was purified by column chromatography on silica gel with hexane/dichloromethane (5:1, v/v) to give a gray solid (540 mg) with a yield of 90%. ^{1}H NMR (400 MHz, CD_2Cl_2) δ 7.50 (m, 4 H), 7.40 (m, 2 H), 7.28 (d, 2 H, J = 8.4 Hz), 7.16 (m, 4 H), 7.08 (m, 2 H), 4.01 (m, 8 H), 1.82 (m, 8 H), 1.44 (m, 28 H), 0.97 (m, 14 H) ppm; 13C NMR (101 MHz, CD_2Cl_2) δ 159.8, 157.0, 147.2, 145.5, 133.6, 132.0, 130.7, 130.3, 125.0, 123.8, 122.6, 114.3, 105.4, 100.2, 99.8, 68.0, 31.6, 29.2, 25.6, 22.7, 13.9 ppm. HRMS (MALDI-TOF), m/z (M^+): for $C_{54}H_{70}BrNO_4$ calculated 875.4488; found 875.4468.

N-(2',4'-bis(hexyloxy)-[1,1'-biphenyl]-4-yl)-2',4'-bis(hexyloxy) -N-(4-(4,4,5,5-tetramethyl-1,3,2-dioxaborolan-2-yl)phenyl)-[1,1'-biphenyl]-4-amine (6). N-(2',4'-bis(hexyloxy)-[1,1'-biphenyl]-4-yl)-N-(4-bromophenyl)-2',4'-bis(hexyloxy)-[1,1'-biphenyl]-4-amine **5** (3.7 g, 4.22 mmol) and bis(pinacolato)diboron (1.2 g, 4.64 mmol) were degassed in 1,4-dioxane (40 mL) together with KOAc (1.242 g, 12.66 mmol) for 30 min. A catalytic amount of $PdCl_2$(dppf) (110 mg, 0.15 mmol) was added, and the reaction mixture was stirred overnight at 85 °C under argon. Ethyl acetate (40 mL) was added to the mixture. The organic layer was washed twice with H_2O and dried over $MgSO_4$, and the solvent was evaporated in Vacuum. Purification by column chromatography (silica gel eluted by DCM containing 25% hexane) yielded 7 (2.924 g, 75%) as a yellow, viscous oil. ^{1}H NMR (400 MHz, CD_2Cl_2) δ 7.75 (d, J =8.4 Hz, 2 H), 7.57 (d, J =8.4 Hz, 4 H), 7.34 (d, J =8.4 Hz, 2 H), 7.20 (m, 6 H), 6.62 (m, 4 H), 4.03 (m, 8 H), 1.85 (m, 8 H), 1.45 (m, 39 H), 1.00 (m, 12 H) ppm. ^{13}C NMR (101 MHz, CD_2Cl_2) δ 160.2, 157.4, 151.1, 145.9, 136.2, 134.2, 131.2, 130.7, 124.8, 123.1, 121.9, 105.9, 100.6, 83.9, 68.8, 68.6, 32.0, 29.7, 27.4, 26.2, 25.3, 25.1, 23.1, 14.3 ppm. HRMS (MALDI-TOF), m/z (M^+): for $C_{60}H_{82}BNO_6$ calculated 923.6235; found 923.6214.

6-(4-(bis(2',4'-bis(hexyloxy)-[1,1'-biphenyl]-4-yl)amino) -phenyl)-4,4-didodecyl-4H-cyclopenta[1,2-b:5,4-b']dithiophene -2-carbaldehyde (7). 6-bromo-4,4-didodecyl-4*H*-cyclopenta[1,2-*b*:5,4-*b'*]dithiophene-2-carbaldehyde (261 mg, 0.42 mmol), **6** (369 mg, 0.4 mol), K_2CO_3 solution 2M (8 ml) and $Pd(PPh_3)_4$ (40 mg) were reacted via Suzuki coupling. Purification using hexane/ DCM (1:1 v/v) as eluent yielded 9a (423 mg, 79%) as a red oil. ^{1}H NMR (400 MHz, CD_2Cl_2) δ 9.73 (s, 1 H), 7.50 (s, 1 H), 7.45 (d, J =8.4 Hz, 2 H), 7.39 (d, J =8.4 Hz, 4 H), 7.17 (d, J =8.4 Hz, 2 H), 7.10 (s, 1 H), 7.08 (d, J =8.4 Hz, 6 H), 6.45 (m, 4 H), 3.89 (m, 8 H), 1.84 (m, 4 H), 1.69 (m, 9 H), 1.38 (m, 9 H), 1.26 (m, 18 H), 1.13 (m, 39 H), 0.79 (m, 21 H). ^{13}C NMR (101 MHz, CD_2Cl_2) δ 182.7, 164.1, 160.2, 157.9, 157.4, 149.8, 148.3, 145.8, 143.4, 134.1, 131.2, 130.7, 128.4, 126.6, 124.5, 123.6, 123.0, 117.2, 105.8, 100.5, 100.5, 68.6, 38.1, 38.1, 32.3, 32.1, 31.9, 30.4, 30.0, 29.8, 29.5, 26.2, 25.0, 23.0, 14.3. HRMS (MALDI-TOF), m/z (M^+): for $C_{88}H_{123}NO_5S_2$ calculated 1337.8843; found 1337.8826.

(E)-3-(6-(4-(bis(2',4'-bis(hexyloxy)-[1,1'-biphenyl]-4-yl)amino) phenyl)-4,4-didodecyl-4H-cyclopenta[1,2-b:5,4-b']dithiophen-2-yl)-2-cyanoacrylic acid (G220). Compound **7** (300 mg, 0.224 mmol), 2-cyanoacetic acid (57.2 mg, 0.672 mmol), and piperidine (133.54 mg, 1.57 mmol) were dissolved in $CHCl_3$ (30 mL). The reaction mixture was heated in a sealing tube at 85°C overnight. The mixture was cooled to room temperature, $CHCl_3$ the aqueous layer was extracted with $CHCl_3$ was washed with 1n HCl, water, and brine and dried with Na_2SO_4 product was purified by silica gel column chromatography using CH_2Cl_2/CH_3OH (v/v=9:1) as eluent to give product as purple solid (151.2 mg) after removal of volatiles under reduced pressure, yield 48%. ^{1}H NMR (400 MHz, CD_2Cl_2) δ 8.39 (s, 1H), 7.67 (s, 1 H), 7.59 (d, J=8.5 Hz, 2 H), 7.53 (d, J= 8.8 Hz, 4 H), 7.31 (d, J=8.6 Hz, 2 H), 7.25 (s, 1 H), 7.20 (m, 7 H), 6.60 (m, 4 H), 4.04 (m, 8 H), 1.97 (m, 4 H), 1.82 (m, 9 H), 1.51 (m, 9 H), 1.38 (m, 20 H), 1.22 (m, 36 H), 0.93 (m, 22 H). ^{13}C NMR (101 MHz, CD_2Cl_2) δ 176.5, 168.8, 165.7, 160.2, 158.8, 157.4, 152.0, 148.7, 145.7, 136.2, 134.3, 130.7, 128.0, 126.8, 124.6, 123.0, 117.2, 105.9, 100.6, 92.0, 68.8, 68.6, 38.2, 32.3, 29.8, 26.2, 25.0, 23.0, 20.8, 14.3. HRMS (MALDI-TOF), m/z (M^+): for $C_{91}H_{124}N_2O_6S_2$, calculated 1404.8901; found 1404.8912.

4-(bis(2',4'-bis(hexyloxy)-[1,1'-biphenyl]-4-yl)amino)benzalde -hyde (4). In a 25 mL single-neck round-bottom flask, 0.269 gram of 4-bromobenzaldehyde (1.45 mmol), 10.42 grams of Bis(2',4'-bis(hexyloxy)-[1,1'-biphenyl]-4-yl)amine (1.38 mmol), and 0.587 gram tribasic potassium phosphate (2.76 mmol) were dissolved in 6 mL of dioxane. This solution was degassed for 20 minutes with a stream of N_2, after which time 10 mg of Pd_2dba_3 and 20 mg of X-Phos were added simultaneously, in one batch. The reaction was then brought to 75 °C for 10 hours. The reaction was then cooled to RT, and plugged through a thin pad of $MgSO_4$

with DCM. The crude product was purified with gradient silica gel chromatography: a gradient from 100% hexanes to 100% DCM. 1.05 grams (83% yield) of a pure yellow oil was obtained. ^{1}H NMR (400 MHz, CD_2Cl_2) δ 9.80 (s, 1H), 7.68 (d, J = 8.8 Hz, 2H), 7.54 (d, J = 8.5 Hz, 4H), 7.24 (dd, J = 15.5, 8.8 Hz, 6H), 7.10 (d, J = 8.7 Hz, 2H), 6.59 – 6.48 (m, 4H), 4.01 (td, J = 6.5, 4.4 Hz, 8H), 1.87 – 1.70 (m, 8H), 1.53 – 1.26 (m, 24H), 1.02 – 0.80 (m, 12). ^{13}C NMR (101 MHz, CD_2Cl_2) δ 190.03, 159.92, 156.97, 153.36, 144.15, 135.47, 131.01, 130.81, 130.57, 128.94, 125.65, 122.24, 119.05, 105.42, 100.10, 68.36, 68.12, 31.59, 31.43, 29.26, 29.05, 25.74, 25.70, 22.62, 22.56, 13.80, 13.78

(E)-3-(4-(bis(2',4'-bis(hexyloxy)-[1,1'-biphenyl]-4-yl)amino) phenyl)-2-cyanoacrylic acid (NT35). The synthesis method resembles that of compound **NT35** to yield 550 mg (51% yield) of red solid. ^{1}H NMR (400 MHz, CD_2Cl_2) δ 8.14 (s, 1H), 7.90 (d, J = 9.1 Hz, 2H), 7.56 (d, J = 8.5 Hz, 4H), 7.31-7.20 (m, 6H), 7.07 (d, J = 9.0 Hz, 2H), 6.63-6.51 (m, 4H), 3.98 (td, J = 6.5, 4.5 Hz, 8H), 1.85-1.68 (m, 8H), 1.56-1.22 (m, 24H), 1.00-0.79 (m, 12H). m/z (M^+): for $C_{58}H_{72}N_2O_6$, calculated 892.5390; found 892.5385.

4-(bis(4-(hexyloxy)phenyl)amino)benzaldehyde (8)

The synthesis method resembles that of compound **4** to yield 550 mg (51% yield) of red solid. ^{1}H NMR (400 MHz, CD_2Cl_2) δ 8.14 (s, 1H), 7.90 (d, J = 9.1 Hz, 2H), 7.56 (d, J = 8.5 Hz, 4H), 7.31-7.20 (m, 6H), 7.07 (d, J = 9.0 Hz, 2H), 6.63-6.51 (m, 4H), 3.98 (td, J = 6.5, 4.5 Hz, 8H), 1.85-1.68 (m, 8H), 1.56-1.22 (m, 24H), 1.00-0.79 (m, 12H). m/z (M^+): for $C_{58}H_{72}N_2O_6$, calculated 892.5390; found 892.5385.

(E)-3-(4-(bis(4-(hexyloxy)phenyl)amino)phenyl)-2-cyano acrylic acid(G221)

The synthesis method resembles that of compound **NT35** to yield 550 mg (51% yield) of red solid. ^{1}H NMR (400 MHz, CD_2Cl_2) δ 8.14 (s, 1H), 7.90 (d, J = 9.1 Hz, 2H), 7.56 (d, J = 8.5 Hz, 4H), 7.31-7.20 (m, 6H), 7.07 (d, J = 9.0 Hz, 2H), 6.63-6.51 (m, 4H), 3.98 (td, J = 6.5, 4.5 Hz, 8H), 1.85-1.68 (m, 8H), 1.56-1.22 (m, 24H), 1.00-0.79 (m, 12H). m/z (M^+): for $C_{58}H_{72}N_2O_6$, calculated 892.5390; found 892.5385.

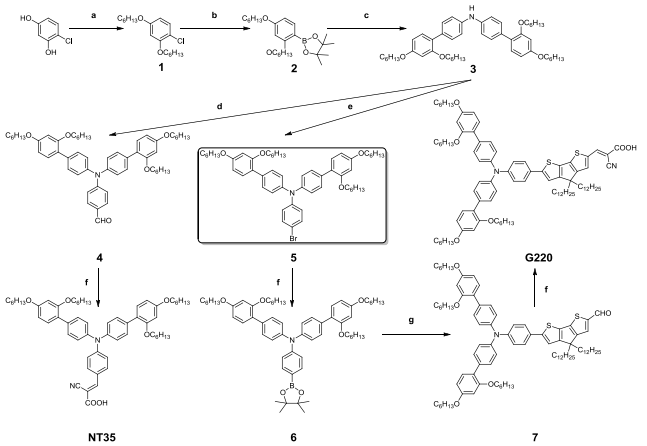

Scheme 1. Synthesis of BPTPA donor **5** and dyes **NT35** and **G220**. Reagents and conditions: (a) $C_6H_{13}Br$, DMF, K_2CO_3, 80°C, 16 h; (b) B_2Pin_2, 1,4-dioxane, KO*t*Bu, $Pd_2(dba)_3$, xPhos, 80°C, 12 h; (c) $Pd(PPh_3)_4$, K_2CO_3 (2M), Toluene, bis(4-bromophenyl)amine,110°C, 12 h; (d) 4-bromobenzaldehyde, tribasic potassium phosphate, 1,4-dioxane, Pd_2dba_3, X-Phos; (e) 1-bromo-4-iodobenzene, 1,4-dioxane, 110°C, 16 h, 90%; (f) 2-cyanoacetic acid, piperidine, chloroform; (g) $Pd(PPh_3)_4$, K_2CO_3 (2M), Toluene, 6-bromo-4,4-didodecyl-4H-cyclopenta[1,2-*b*:5,4-*b'*]dithiophene-2-carbaldehyde, 110°C, 12 h.

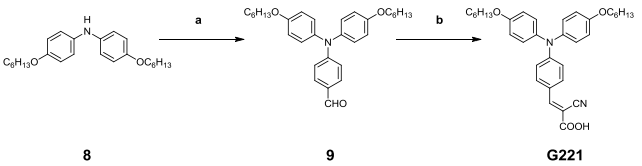

Scheme 2. Synthesis of **G221**. Reagents and conditions: (a) 4-bromobenzaldehyde, tribasic potassium phosphate, 1,4-dioxane, Pd_2dba_3, X-Phos; (b) 2-cyanoacetic acid, piperidine, chloroform.

Device fabrication

A screen-printed double layer of nanocrystalline TiO_2 particles was used as the photoelectrode. The FTO glass plates were immersed into a 40 mM aqueous $TiCl_4$ solution at 70 °C for 30min and washed with water and ethanol. A 7 microns thick film of 20 nm-sized TiO_2 particles[27] was then printed on the FTO conducting glass and further coated with a 4 microns thick second layer of 400 nm light-scattering TiO_2 particles (400 nm diameter, Catalysts & Chemicals Ind. Co. Ltd. (CCIC), HPW-400). Sintering was carried out at 500 °C for 15 min, which was gradually heated. The films were heated again at 500 °C for 30 min followed by cooling to 80 °C and dipping into a 0.1 mM solution of dyes in a mixture of acetonitrile and tertbutyl alcohol (volume ratio, 1:1) for 15 h at room temperature. To prepare the counter electrode, Pt catalyst was deposited on cleaned FTO glass by coating with a drop of H_2PtCl_6 solution (10 mM in 2-propanol solution) with heat treatment at 400 °C for 15 min. For the assembly of DSSCs, the dye-contained TiO_2 electrode and Pt counter electrode were assembled into a sandwich-type cell and sealed with a hot-melt gasket of 25 microns thickness made of the ionomer Surlyn 1702 (Dupont). The redox electrolyte was placed in a drilled hole in the counter electrode, and was driven into the cell by means of vacuum backfilling. Two types of electrolytes were used for device evaluation, in which **JH34** was composed of 0.6 M DMII, 0.05 M LiI, 0.03 M I_2, 0.25 M TBP, 0.05 M GuNCS as the iodine electrolyte, and **JH180** was composed of 0.22M Co^{2+}, 0.05 M Co^{3+}, 0.1 M $LiClO_4$, 0.2 M TBP as the cobalt electrolyte. Finally, the hole was sealed using Surlyn and a cover glass (0.1 mm thickness).

Photovoltaic properties measurements

Photovoltaic measurements employed an AM 1.5 solar simulator equipped with a 450 W xenon lamp (Oriel, USA). The spectral output of the lamp was matched in the region of 350–750 nm with the aid of a Schott K113 Tempax sunlight filter (Präzisions Glas & Optik GmbH, Germany) so as to reduce the mismatch between the simulated and true solar spectra to less than 4%. I–V curves were obtained by applying an external bias to the cell and measuring the generated photocurrent with a Keithley model 2400 digital source meter. The voltage step 10mV was kept and delay time of the photocurrent was and 40 ms and 80 ms for iodine based and cobalt based electrolyte, respectively. The photocurrent action spectra were measured with the Incident Photon-to-Current conversion Efficiency (IPCE) test system. The modulation frequency used was about 2 Hz and light from a 300 W Xenon lamp (ILC Technology, USA) was focused through a computer controlled Gemini-180 double monochromator (John Yvon Ltd., UK). A white light bias was used to bring the total light intensity on the device under test closer to operating

conditions. The devices were masked to attain an illuminated active area of 0.2 cm^2.

Photovoltage Transient Measurements

Photovoltage transients were observed by using a pump pulse generated by four red light emitting diodes controlled by a fast solid-state switch with a white light bias. The pulse of red light with widths of 100 ms was incident on the photoanode side of the cell, and its intensity was controlled to keep a suitably low level to generate the exponential voltage decay where the charge recombination rate constants are obtained directly from the exponential decay rate. A white bias light, also incident on the same side of the device, was supplied by white diodes. Small perturbation transient photocurrent measurements were performed in a similar manner to the open-circuit voltage decay measurement.

Results and Discussion

Synthesis

The uniqueness of the BPTPA donor lie in the two additional bis(hexyloxy)benzene substitutes on a normal TPA structure, which are supposed to not just improve the solubility, but also decrease electron recombination and enhance the open circuit voltage especially in the presence of cobalt complex redox shuttle. One improved synthetic route to BPTPA donor **6** is depicted in Scheme 1. Starting from cheap chlororesorcinol, hexyl chains were introduced through electronphilic substitution. Then the chloride is substituted by pinacol boronic ester using Buchwald catalyst system to get compound **2**. Through the Suzuki reactions between **2** and bis(4-bromophenyl)amine, the route led to BPDPA donor **3**, which can be converted to standard BPTPA donor **5** via CuI catalyzed amination reaction in high yield. By adopting the new route, the overall yield of **5** increased to 63% over four steps comparing to 11% over six steps in the old synthetic route.[20] After the conversion of **5** to its Bpin derivative **6**, a Suzuki coupling reaction with 6-bromo-4,4-didodecyl-cyclopentadithiophene-2-carbaldehyde give the aldehyde precursor **7**. Finally, the conventional Knoevenagel condensation yielded dye **G220** with cyanoacetic acid in the presence of piperidine. Conjugation length can be further tailored by reacting compound **3** with 4-Bromobenzaldehyde to afford monoaldehyde precursors **4**. In the end, a shortened version of **D35** called **NT35** was obtained following the same reaction condition as making **G220**. From a structural point of view, **NT35** is like the BPTPA donor itself with electron acceptor or **D35** without a thiophene bridge. When the thiophene in **D35** is replaced by an alkylated cyclopentadithiophene (CPDT), **G220** is synthesized. For the reason of comparison, **G221** with simple TPA connecting directly to the anchor group was also synthesized. These dyes and their precursor compounds are well soluble in common organic solvents (i.e., chloroform, DMF, and THF). The structure and purity of the four compounds were confirmed by standard spectroscopic methods.

Spectral properties

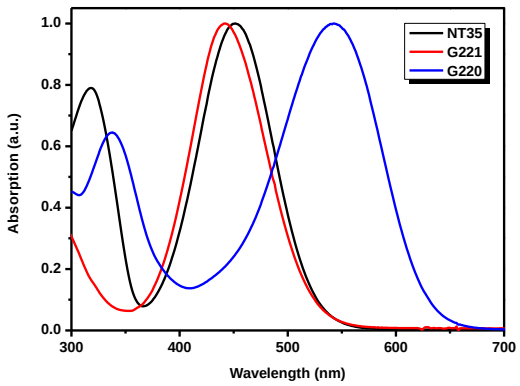

Figure 3. UV-Vis absorption spectra of the three dyes in CH_2Cl_2 solutions

The UV-Vis absorption spectra of the three dyes (**NT35**, **G220** and **G221**) in CH_2Cl_2 solutions are shown in Figure 3, and their absorption peaks as well as their extinction coefficients are summarized in Table 1. According to the UV-Vis spectra, these dyes exhibit two major prominent bands, appearing at ca. 300–380 nm and ca. 400–650 nm respectively. The absorption bands in the UV region can be assigned to a localized aromatic π-π* transition, while the absorption bands in the visible region originate from an intramolecular charge transfer (ICT) transition between the triphenylamine donor part and the acceptor. For the charge-transfer band, the absorption maxima vary according to different donor substitution and conjugated bridges (441 nm for **G221**, 451 nm for **NT35** and 542 nm for **G220**). The absorption of **NT35** with BPTPA donor is 10 nm red shifted than that of **G221** with normal TPA. Compared with **G221** and **NT35**, the absorption band of **G220** shows considerably large red-shift (91 nm) due to the greater electron-donating ability of the CPDT unit in the π-bridge of this dye, which further decreases the band gap and results in a broader ICT band region. This trend is in accord with the conjugation length and electron richness of the bridge unit, illustrating that the modulation of the optical band-gaps and energy levels of these sensitizers can be partly achieved by altering the electronic nature of the π-conjugation bridges.

Table 1. Absorbance and electrochemical properties of dyes

dye	λ_{max} (nm)[a]	$\varepsilon \cdot 10^4$ (M^{-1} cm^{-1})	E_{ox} (V)[b] vs NHE	$E_{0\text{-}0}$ (V)[c]	E_{ox}-$E_{0\text{-}0}$ (V) vs NHE	HOMO /LUMO (eV)[d]
NT35	451	3.04	1.04	2.39	-1.35	-5.54/-3.15
G220	542	5.27	0.90	1.99	-1.09	-5.40/-3.41
G221	441	2.64	1.11	2.40	-1.29	-5.61/-3.21

[a] Measured in 2 × 10^{-6} M of CH_2Cl_2 solutions at room temperature. [b] Measured in CH_2Cl_2 containing 0.1 M of tetra-n-butylammonium hexafluorophosphate ($TBAPF_6$) electrolyte (working electrode: glassy carbon; counter electrode: Pt; reference electrode: Pt; calibrated with ferrocene/ferrocenium (Fc/Fc+) as an internal reference and converted to NHE by addition of 630 mV).[28] [c] Estimated from onset wavelength in absorption spectra. [d] NHE vs. the vacuum level is set to 4.5 V.[29]

Electrochemical properties

To estimate the HOMO level of the dyes, cyclic voltammetry was

employed using a three-electrode cell with 0.1 M $TBAPF_6$ in CH_2Cl_2 as the supporting electrolyte. The cyclic voltammetry (CV) diagrams of the dyes are shown in Figure 4, and the corresponding data are listed in Table 1.

It is shown that the first oxidation potentials (E_{ox}) corresponding to the highest occupied molecular orbitals (HOMOs) levels of the dyes (NT35: 1.11 V, G220: 0.90 V and G221: 1.04 V) are sufficiently more positive than the I^-/I_3^- redox potential value (0.35 V vs. NHE) and $[Co(bpy)_3]^{3+/2+}$ redox potential value (0.49 V vs. NHE)[20], indicating that the oxidized dyes formed after electron injection into the conduction band of TiO_2 could be efficiently regenerated by means of reaction with the redox couples thermodynamically.

Except **G221**, two oxidation waves were generally observed in the voltammograms with the other two dyes. The first quasi-reversible oxidation wave at lower oxidation potentials is attributed to the triphenylamine, whereas the higher oxidation potentials with quasi-reversible behavior were from the respective π bridges. **G220** has the lowest oxidation potential because the oxidized triphenylamine can be stabilized by the electron-rich CPDT unit nearby, and the highest oxidation potential of **G221** is ascribed to the lack of both bis(hexyloxy)benzene and a π bridge. The lower oxidation potentials means the HOMO raising upon the introduction of stronger electron donating moieties, which agrees well with the molecular structure. The reduction potentials corresponding to the lowest unoccupied molecular orbital (LUMO) levels of these dyes (described as $E_{red} = E_{ox} - E_{0\text{-}0}$, see Table 1) were more negative than E_{cb} (conduction band edge energy level) of the TiO_2 electrode (-0.5 V vs NHE),[30] hence, an effective electron transfer is energetically possible from the excited dye to the conduction band (CB) of TiO_2.

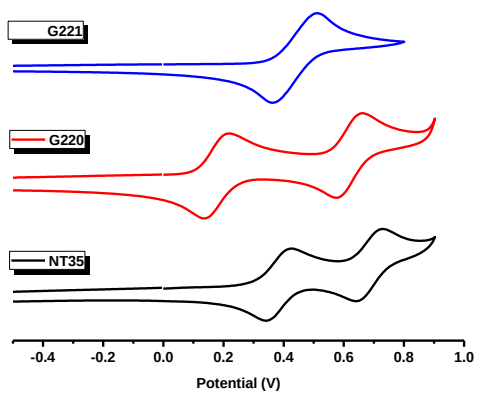

Figure 4. Cyclic voltammograms of the dyes in CH2Cl2 solutions.

To scrutinize the electronic properties of these dyes further, the optimized structures and electron distribution of the HOMOs and LUMOs of **NT35**, **G220** and **G221** performed by density functional theory (DFT) at the B3LYP/6-31G* level in the gas phase are shown in Figure SX. In all the four dyes, the electron density of the HOMOs are primarily located on the π-framework of the donor part (TPA), whereas the electron density of the LUMOs primarily extended throughout the cyanoacrylic acid acceptor and the neighboring π bridges. Thus, the strong electron density relocation between HOMO and LUMO is present and ensuring a strong coupling of the dye excited state with the semiconductor surface.

Photovoltaic performance of DSSCs

To compare the performance of the synthesized dyes in Co^{3+}/Co^{2+} electrolyte and I_3^-/I^- redox system, hence to evaluate the potential of the BPTPA donor, DSSCs with two different kinds of redox shuttles were fabricated for each dye with the same double-layer TiO_2 as photoanode and Pt-coated glass as the counter electrode.

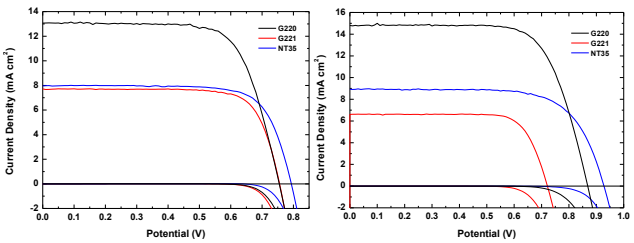

Figure 5. *J-V* curves of DSSCs sensitized with the dyes with (a) iodine and (b) cobalt as a redox couple, respectively.

Figure 6 shows the incident photon-to-electron conversion efficiency (IPCE) as a function of incident wavelength for DSSCs based on these dyes in Co^{3+}/Co^{2+} and I_3^-/I^- redox couple. As is shown in Figure 6a, with I_3^-/I^- redox system, the solar cells based on **NT35** and **G221** show similar spectral responses and high IPCEs above 80% in the range of 450-510 nm. Meanwhile, although much broader absorption was observed with **G220**, its IPCE value is almost completely lower than 80% in the range of 400-680 nm. Such broader spectral response of **G220** is consistent with the trend of the absorption spectra, implying its better light harvesting ability for long-wavelength visible lights, which would be attributed to the larger CPDT π system. At the same time, when all the parameters are kept except that the electrolyte is changed to Co^{3+}/Co^{2+} redox system, the IPCE spectral responses of BPTPA donor substituted **NT35** and especially **G220** are improved evidently below 450 nm, possibly due to the lack of competitive light absorption by triiodide, which lowered the IPCE of the iodine system relative to that of the cobalt system. (Figure 6b) On the contrary, the spectral response of **G221** is much deteriorated, indicating that the **G221** sensitized TiO_2 electrode would generate the lowest conversion yield among the three dyes. Considering the only structural difference between **G221** and **NT35** lie in the BPTPA donor, this example directly proved the compatibility of BPTPA donor with cobalt electrolyte.

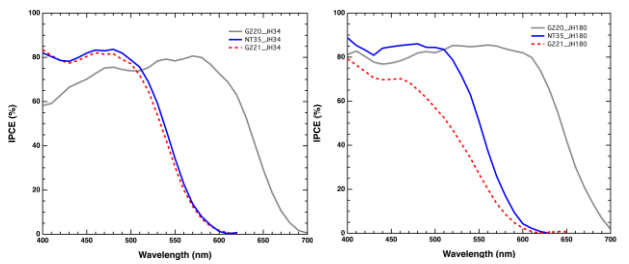

Figure 6. IPCE spectra of DSSCs sensitized with the dyes with (a) iodine and (b) cobalt as a redox couple, respectively.

Figure 5a and 5b show the current–voltage characteristics of

the DSSCs fabricated with **NT35**, **G220** and **G221** as sensitizers under standard global AM 1.5 solar light conditions in cobalt electrolyte and iodine electrolyte respectively. The detailed parameters of shortcircuit current density (J_{sc}), open-circuit voltage (V_{oc}), fill factor (*FF*), and photovoltaic conversion efficiency (μ) are summarized in Table 2. In both redox systems, J_{sc} data are positively proportional to the absorption width of the dye molecules. For example, **G220** dye has the broadest light harvesting range and consequently the highest J_{sc}. **NT35** has higher V_{oc} than that of **G221** in both redox systems because the introduction of bulky BPTPA donor can act as barriers preventing electrolyte from approaching the TiO_2 surface, inhibiting charge recombination, which is more explicit in cobalt electrolyte.

For **NT35** and **G220**, the J_{sc} values of the cells with the cobalt electrolyte were around 12% higher than that of the iodine-based DSSCs. This increase was also reflected on the IPCE curves and could be ascribed to the lack of competitive light absorption by iodine electrolyte. It is noteworthy that the two dyes with BPTPA donor (**NT35** and **G220**) all have higher open circuit voltages (V_{oc}) (928 mV and 868 mV) in cobalt electrolyte than in iodine electrolyte (793 mV and 755 mV) measured under the same conditions and the increase was ascribed mainly to a 210 mV negative shift of the redox potential of the cobalt complex.[20] Whereas, both the J_{sc} and V_{oc} of **G221** cell with cobalt redox shuttle are lower than that of the same cell with an iodine electrolyte system. (Figure 5, Table 2) This result is in agreement with previous investigations,[17] and was interpreted by rapid recombination from electrons in the TiO_2 conduction band to the cobalt(III) species. While in this study, BPTPA donor showed again tangible effect in solving this problem. That is to say by introducing the BPTPA donor we can fully make use of the advantageous tunable redox potential of cobalt electrolyte without worrying about the adverse charge recombination. Consequently, the cell based on **G220** dye showed the best photovoltaic performance in both iodine electrolyte (6.97 %) and cobalt electrolyte (8.61 %). With relatively lower J_{sc}, solar cells based on **NT35** and **G221** show relatively inferior efficiencies (Table 2). This result indicates that the BPTPA donor is beneficial for cobalt-based DSSCs and provides a strategy to construct dye molecules that can work with iodine-free electrolytes as well as Iodine electrolyte.

Table 2. Photovoltaic performance of DSSCs Sensitized with **NT35**, **G220** and **G221** in Iodine and cobalt Electrolytes

dye	electrolyte	J_{sc} (mA/cm^2)	V_{oc} (mV)	*FF*	η (%)
NT35	Iodine	7.96	793	0.744	4.70
	Cobalt	8.92	928	0.701	5.80
G220	Iodine	13.1	755	0.707	6.97
	Cobalt	14.8	868	0.705	9.06
G221	Iodine	7.71	756	0.758	4.42
	Cobalt	6.61	721	0.765	3.62

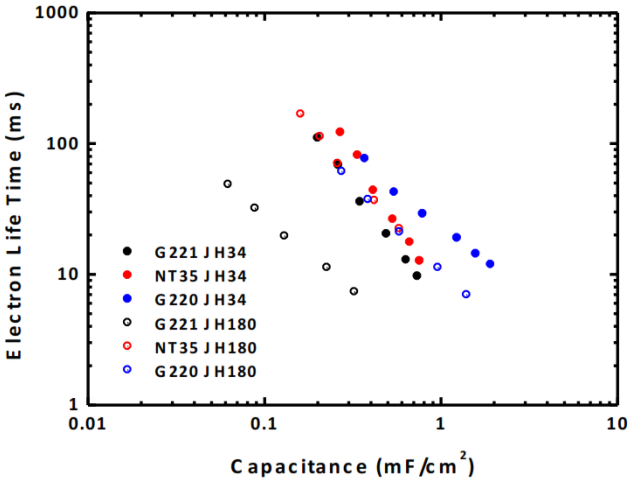

Figure 7. Dependence of TiO_2 electron lifetimes on capacitance as recorded from photocurrent decay measurements for the investigated dyes.

To provide a rationale for the origin of the different V_{oc} shift behavior observed when employing cobalt- and iodine based electrolytes, dependence of TiO_2 electron lifetimes on capacitance as recorded from photocurrent decay measurements for the investigated dyes were measured (Figure 7). After the introduction of BPTPA donor, **NT35**- and **G220** based DSSCs showed much longer electron lifetimes and no significant change in the electron lifetime in both cobalt- and iodine based electrolytes, while iodine-based devices show slightly longer electron lifetimes though. By contrast, a striking difference is observed for the **G221** dye, which showed the largest drop of electron lifetimes with the cobalt-based electrolyte compared to iodine-based devices, indicating that the recombination reaction between the electrons on the TiO_2 surface and the trivalent cobalt complex in the electrolyte was considerably faster than that of an iodine-based device. Furthermore, DSSCs based on the **G221** dye in conjunction with the iodine electrolytes, on the other hand, showed shortest electron lifetimes among all the devices of the same type too. This result is also supported by the changes in the dark current with applied bias, which is indicative of the electron recombination rate with the electrolyte. (Figure 5) The onset of recombination current occurs at the lowest potential for **G221** compared to the other two dyes in cobalt electrolyte. (Figure 5b) The observed increase in dark current density of **G221** is essentially due to the deficient suppression of Co^{3+} reduction at the dye-sensitized TiO_2 electrode. At the same time, the dyes with BPTPA donor all had relatively lower dark current density. To conclude, we developed a simple, feasible approach to the construction of dyes compatible with cobalt-based systems and confirmed that the use of BPTPA donor is ideal for suppressing recombination reaction especially in cobalt-based DSSCs.

Conclusions

To summary, we have developed a simplified synthesis of BPTPA donor from chlororesorcinol in an overall yield of 63% over four steps for the DSSC donor unit. To further validate the functionality of this donor group in working with Co^{3+}/Co^{2+} redox couple, two new organic D-π-A dye **NT35** and **G220** containing BPTPA donor and exhibiting different IPCE spectrum response were synthesized. **G221** with just a TPA as the donor

unit was also made for comparison reason. The combination of the sensitizers bearing BPTPA donor with cobalt complex showed higher J_{sc}, V_{oc} and better visible light spectrum response than that of the combinations with Iodine electrolyte. Compared with **NT35**, **G221** without BPTPA donor exhibited depreciated performance in both Iodine and cobalt electrolytes. This result indicate that the BPTPA donor could efficiently suppress the electron recombination between the TiO_2 surface and the redox oxide species. The DSSC made by **G221** showed even worse V_{oc} in cobalt electrolyte than in Iodine electrolyte. With respect to **NT35**, the **G220** dye with CPDT as the π bridge, when combined with the cobalt electrolyte evokes a dramatic red-shifted photocurrent response and the photovoltaic performance is consistent entirely. Therefore, **G220** based cell shows the best light to electricity conversion efficiency of 8.61% (J_{sc} = 14.27 mA cm^{-2}, V_{oc} = 0.88 V, *FF* = 0.68) with cobalt electrolyte. In view of the excellent compatibility of BPTPA donor with cobalt electrolyte, it is believed that the much-improved synthetic route could make it possible to scale up the production of iodine-free dye-sensitized solar cells.

Acknowledgment. This work was supported by FP7-ENERGY-2010 project 261920 "ESCORT" and FP7/2007-2013 under grant agreement n° 246124 of the SANS project for financial support. MKN thanks World Class University program, Photovoltaic Materials, Department of Material Chemistry, Korea University, Chungnam, 339-700, Korea.

Notes and references

[a] *Laboratory for Photonics and Interfaces, Institution of Chemical Sciences and Engineering, School of Basic Sciences, Swiss Federal Institute of Technology, CH-1015 Lausanne, Switzerland.*
E-mail: xxxx@aaa.bbb.ccc
[b] *R & D Center DSC Team, Dongjin Semichem Co., LTD. 445-935 Hwasung, South Korea*

† Electronic Supplementary Information (ESI) available: DFT calculation results. See DOI: 10.1039/b000000x/

1 (a) A. Mishra, M. K. R. Fischer, and P. Bauerle, *Angew. Chem., Int. Ed.*, 2009, **48**, 2474; (b) H. Qin, S. Wenger, M. Xu, F. Gao, X. Jing, P. Wang, S. M. Zakeeruddin, and M. Grätzel, *J. Am. Chem. Soc.*, 2008, **130**, 9202; (c) H. Y. Yang, Y. S. Yen, Y. C. Hsu, H. H. Chou, and J. T. Lin, *Org. Lett.*, 2010, **12**, 16; (d) T. Bessho, S. M. Zakeeruddin, C.-Y. Yeh, E. W.-G. Diau, and M. Grätzel, *Angew. Chem., Int. Ed.*, 2010, **49**, 6646; (e) T. Daeneke, T.-H. Kwon, A. B. Holmes, N. W. Duffy, U. Bach, and L. Spiccia, *Nat. Chem.*, 2011, **3**, 211.

2 (a) S. Hwang, J. H. Lee, C. Park, H. Lee, C. Kim, C. Park, M.-H. Lee, W. Lee, J. Park, K. Kim, N.-G. Park, and C. Kim, *Chem. Commun.*, 2007, 4887; (b) D. P. Hagberg, J.-H. Yum, H. Lee, F. De Angelis, T. Marinado, K. M. Karlsson, R. Humphry-Baker, L. Sun, A. Hagfeldt, M. Grätzel, and M. K. Nazeeruddin, *J. Am. Chem. Soc.*, 2008, **130**, 6259; (c) W.-H. Liu, I. C. Wu, C.-H. Lai, C.-H. Lai, P.-T. Chou, Y.-T. Li, C.-L. Chen, Y.-Y. Hsu, and Y. Chi, *Chem. Commun.*, 2008, 5152; (d) K. R. Justin Thomas, Y.-C. Hsu, J. T. Lin, K.-M. Lee, K.-C. Ho, C.-H. Lai, Y.-M. Cheng, and P.-T. Chou, *Chem. Mater.* 2008, **20**, 1830; (e) J.-H. Yum, D. P. Hagberg, S.-J. Moon, K. M. Karlsson, T. Marinado, L. Sun, A. Hagfeldt, M. K. Nazeeruddin, and M. Grätzel, *Angew. Chem., Int. Ed.*, 2009, **48**, 1576.

3 (a) K. Hara, K. Sayama, H. Arakawa, Y. Ohga, A. Shinpo, and S. Suga, *Chem. Commun.*, 2001, 569; (b) K. Hara, M. Kurashige, Y. Dan-oh, C. Kasada, A. Shinpo, S. Suga, K. Sayama, and H. Arakawa, *New J. Chem.*, 2003, **27**, 783; (c) K. Hara, T. Sato, R. Katoh, A. Furube, Y. Ohga, A. Shinpo, S. Suga, K. Sayama, H. Sugihara, and H. Arakawa, *J. Phys. Chem. B*, 2003, **107**, 597; (d) K. Hara, Z.-S. Wang, T. Sato, A. Furube, R. Katoh, H. Sugihara, Y. Dan-oh, C. Kasada, A. Shinpo, and S. Suga, *J. Phys. Chem. B*, 2005, **109**, 15476.

4 (a) T. Horiuchi, H. Miura, S. Uchida, *Chem. Commun.*, 2003, 3036; (b) T. Horiuchi, H. Miura, K. Sumioka, and S. Uchida, *J. Am. Chem. Soc.* 2004, **126**, 12218; (c) L. Schmidt-Mende, U. Bach, R. Humphry-Baker, T. Horiuchi, H. Miura, S. Ito, S. Uchida, and M. Grätzel, *Adv. Mater.* 2005, **17**, 813; (d) S. Ito, S. M. Zakeeruddin, R. Humphry-Baker, P. Liska, R. Charvet, P. Comte, M. K. Nazeeruddin, P. Pechy, M. Takata, H. Miura, S. Uchida, and M. Grätzel, *Adv. Mater.*, 2006, **18**, 1202; (e) D. Kuang, S. Uchida, R. Humphry-Baker, S. M. Zakeeruddin, and M. Grätzel, *Angew. Chem., Int. Ed.* 2008, **47**, 1923; (f) S. Ito, H. Miura, S. Uchida, M. Takata, K. Sumioka, P. Liska, P. Comte, P. Pechy, and M. Grätzel, *Chem. Commun.* 2008, 5194.

5 K. Guo, K. Yan, X. Lu, Y. Qiu, Z. Liu, J. Sun, F. Yan, W. Guo, and S. Yang, *Org. lett.*, 2012, **14**, 2214.

6 S. Franco, J. Garín, N. M. de Baroja, R. Pérez-Tejada, J. Orduna, Y. Yu, and M. Lira-Cantú, *Org. lett.* 2012, **14**, 752.

7 W. Zeng, Y. Cao, Y. Bai, Y. Wang, Y. Shi, M. Zhang, F. Wang, C. Pan, and P. Wang, *Chem. Mater*., 2010, **22**, 1915;

8 (a) P. Bonhote, J.-E. Moser, R. Humphry-Baker, N. Vlachopoulos, S. M. Zakeeruddin, L. Walder, and M. Grätzel, *J. Am. Chem. Soc.*, 1999, **121**, 1324; (b) Z. Ning, Q. Zhang, W. Wu, and H. Tian, *J. Org. Chem.* 2008, **73**, 3791.

9 J.-H. Yum, D. P. Hagberg, S. -J. Moon, K. M. Karlsson, T. Marinado, L. Sun, A. Hagfeldt, M. K. Nazeeruddin, and M. Grätzel, *Angew. Chem. Int. Ed.*, 2009, **48**, 1576 .

10 (a) J. E. Kroeze, N. Hirata, L. Schmidt -Mende, C. Orizu, S. D. Ogier, K. Carr, M. Grätzel, and J. R. Durrant, *Adv. Funct. Mater.*, 2006, **16**, 1832; (b) G. Boschloo, T. Marinado, K. Nonomura, T. Edvinsson, A. G. Agrios, D. P. Hagberg, L. Sun, M. Quintana, C. S. Karthikeyan, M. Thelakkat, and A. Hagfeldt, *Thin Solid Films*, 2008, **516**, 7214; (c) C. S. Karthikeyan, H. Wietasch, and M. Thelakkat, *Adv. Mater.* 2007, **19**, 1091.

11 (a) R. Li, J. Liu, N. Cai, M. Zhang, and P. Wang, *J. Phys. Chem. B*, 2010, **114**, 4461; (b) N. Cai, S.-J. Moon, L. Cevey-Ha, T. Moehl, R. Humphry-Baker, P. Wang, S. M. Zakeeruddin, and M. Grätzel, *Nano lett.*, 2011, **11**, 1452.

12 M. Xu, S. Wenger, H. Bala, D. Shi, R. Li, Y. Zhou, S. M. Zakeeruddin, M. Grätzel, and P. Wang, *J. Phys. Chem. C*, 2009, **113**, 2966

13 K. Do, D. Kim, N. Cho, S. Paek, K. Song, and J. Ko, *Org. lett.*, 2012, **14**, 222

14 (a) T. Daeneke, T.-H. Kwon, A. B. Holmes, N. W. Duffy, U. Bach, and L. Spiccia, *Nat. Chem.*, 2011, **3**, 211; (b) S. M. Feldt, E. A. Gibson, E. Gabrielsson, L. Sun, G. Boschloo, and A. Hagfeldt, *J. Am.Chem.Soc.*, 2010, **132**, 16714; (c) D. Zhou, Q. Yu, N. Cai, Y. Bai, Y. Wang, and P. Wang, *Energy Environ. Sci.* 2011, **4**, 2030; (d) Y. Bai, Q. Yu, N. Cai, Y. Wang, M. Zhang, and P. Wang, *Chem. Commun.* 2011, **47**, 4376.

15 H. Nusbaumer, J. E. Moser, S. M. Zakeeruddin, M. K. Nazeeruddin, and M. Grätzel, *J. Phys. Chem. B*, 2001, **105**, 10461.

16 (a) S. A. Sapp, C. M. Elliott, C. Contado, S. Caramori and C. A. Bignozzi, *J. Am. Chem. Soc.*, 2002, **124**, 11215; (b) Y. Bai, J. Zhang, D. Zhou, Y. Wang, M. Zhang, and P. Wang, *J. Am. Chem. Soc.*, 2011, **133**, 11442; (c) J.-H. Yum, E. Baranoff, F. Kessler, T. Moehl, S. Ahmad, T. Bessho, A. Marchioro, E. Ghadiri, J.-E. Moser, C. Yi, M. K. Nazeeruddin, and M. Grätzel, *Nat. comm.*, 2012, **3**, 631; (d) E. Mosconi, J.-H. Yum, F. Kessler, C. J. Gomez-Garcia, C. Zuccaccia, A. Cinti, M. K. Nazeeruddin, M. Grätzel, and F. De Angelis, *J. Am. Chem. Soc.*, 2012, **134**, 19438; (e) C. Qin, W. Peng, K. Zhang, A. Islam, and L. Han, *Org. Lett.* 2012, **14**, 2532.

17 (a) J. J. Nelson, T. J. Amick, and C. M. Elliott, *J. Phys. Chem.C*, 2008, **112**, 18255; (b) B. M. Klahr and T. W. Hamann, *J. Phys. Chem. C*, 2009, **113**, 14040; (c) H. Nusbaumer, S. M. Zakeeruddin, J. E. Moser, M. Gratzel, *Chem. Eur. J.* 2003, **9**, 3756. (d) Y. Liu, J. R.

Jennings, Y. Huang, Q. Wang, S. M. Zakeeruddin, and M. Grätzel, *J. Phys. Chem.C*, 2011, **115**, 18847.
18 D. P. Hagberg, X. Jiang, E. Gabrielsson, M. Linder, T. Marinado, T. Brinck, A. Hagfeldt, and L. Sun, *J. Mater. Chem*, 2009, **19**, 7232.
19 S. M. Feldt, E. A. Gibson, E. Gabrielsson, L. Sun, G. Boschloo, and A. Hagfeldt, *J. Am. Chem. Soc.*, 2010, **132**, 16714.
20 H. N. Tsao, C. Yi, T. Moehl, J.-H. Yum, S. M. Zakeeruddin, M. K. Nazeeruddin, and M. Grätzel, *ChemSusChem*, 2011, **4**, 591.
21 H. N. Tsao, P. Comte, C. Yi, and M. Grätzel, *Chemphyschem*, 2012, 13, 2976.
22 A. Yella, H.-W. Lee, H. N. Tsao, C. Yi, A. K. Chandiran, M. K. Nazeeruddin, E. W.-G. Diau, C.-Y. Yeh, S. M. Zakeeruddin, and M. Grätzel, *Science (New York, N.Y.)*, 2011, **334**, 629.
23 T. W. Hamann, *Dalton trans., (Cambridge, England : 2003)*, 2012, **41**, 3111.
24 (a) A. Hagfeldt and M. Grätzel, *Acc. Chem. Res.*, 2000, **33**, 269; (b) M. Liang, W. Wu, F. Cai, P. Chen, B. Peng, J. Chen and Z. Li, *J. Phys. Chem. C*, 2007, **111**, 4465; (c) W. Xu, B. Peng, J. Chen, M. Liang, and F. S. Cai, *J. Phys. Chem. C*, 2008, **112**, 874.
25 J.-H. Yum, T. W. Holcombe, Y. Kim, J. Yoon, K. Rakstys, M. K. Nazeeruddin, and M. Grätzel, *Chem. Comm.*, 2012, **48**, 10727.
26 M. Shellaiah, Y. C. Rajan, and H.-C. Lin, J.Mater. Chem., 2012, 22, 8976.
27 S. Ito, T. N. Murakami, P. Comte, P. Liska, C. Grätzel, M. K. Nazeeruddin, and M. Grätzel, *Thin Solid Films*, 2008, **516**, 4613.
28 J. Mei, K. R. Graham, R. Stalder, J. R. Reynolds, Org. Lett. 2010, 12, 660.
29 L. Bürgi, M. Turbiez, R. Pfeiffer, F. Bienewald, H.-J. Kirner, and C. Winnewisser, Advanced Materials, 2008, 20, 2217.
30 B. O'Regan and M. Grätzel, *Nature*, 1991, **353**, 737. (b) M. Grätzel, *Nature*, 2001, **414**, 338.